



Large-scale brain organization during facial emotion processing as a function of early life trauma among adolescent girls

Josh M. Cisler^{a,*}, Anthony Privratsky^b, Sonet Smitherman^b, Ryan J. Herringa^a, Clinton D. Kilts^b

^a University of Wisconsin Madison, Department of Psychiatry, United States

^b University of Arkansas for Medical Sciences, Department of Psychiatry, Brain Imaging Research Center, United States

ABSTRACT

Background: A wealth of research has investigated the impact of early life trauma exposure on functional brain activation during facial emotion processing and has often demonstrated amygdala hyperactivity and weakened connectivity between amygdala and medial PFC (mPFC). There have been notably limited investigations linking these previous node-specific findings into larger-scale network models of brain organization.

Method: To address these gaps, we applied graph theoretical analyses to fMRI data collected during a facial emotion processing task among 88 adolescent girls (n = 59 exposed to direct physical or sexual assault; n = 29 healthy controls), aged 11–17, during fMRI. Large-scale organization indices of modularity, assortativity, and global efficiency were calculated for stimulus-specific functional connectivity using an 883 region-of-interest parcellation.

Results: Among the entire sample, more severe early life trauma was associated with more modular and assortative, but less globally efficient, network organization across all stimulus categories. Among the assaulted girls, severity of early life trauma and PTSD diagnoses were both simultaneously related to increased modular brain organization. We also found that more modularized network organization was related both to amygdala hyperactivation and weakened connectivity between amygdala and medial PFC.

Conclusions: These results demonstrate that early life trauma is associated with enhanced brain organization during facial emotion processing and that this pattern of brain organization might explain the commonly observed association between childhood trauma and amygdala hyperactivity and weakened connectivity with mPFC. Implications of these results for neurocircuitry models are discussed.

1. Introduction

Early life trauma is widely recognized as a potent risk factor for subsequent mental health disorders, including posttraumatic stress disorder (PTSD), depression, and substance use disorders (Green et al., 2010; McLaughlin et al., 2010; Felitti et al., 1998). Among the various forms of early life trauma to which one can be exposed, assaultive violence, including physical or sexual assault, confers notably greater risk for negative mental health outcomes (Cisler et al., 2011a,b, 2012). Though the association between early life trauma and risk for mental health disorders has been well established, the brain mechanisms that mediate this association have yet to be clearly defined.

Contemporary neurocircuitry models of trauma and PTSD (Pitman et al., 2012; Rauch et al., 2006; Admon et al., 2013) emphasize hyperactivity of the amygdala and dorsal anterior cingulate cortex (dACC) as neural mediators of hypervigilance to threat and hypoactivity of the hippocampus and medial prefrontal cortex (mPFC) as neural mediators

of emotion regulation/fear extinction deficits and re-experiencing symptoms. It is important to briefly mention that the mPFC is functionally heterogeneous and refers to a broad anatomical space, and in the context of these neurocircuitry models, the mPFC often refers more specifically to the perigenual/ventral ACC (Marusak et al., 2016). While a wealth of data from the past two decades support this model, a more recent focus has been on understanding how these canonical trauma and PTSD-related neural regions fit into larger and well-mapped functional networks (Patel et al., 2012). Indeed, the field of neuroimaging is generally moving away from functional segregation approaches to understanding cognition and mental health disorders and instead moving towards analytic approaches that capture large-scale and distributed properties of information processing in the human brain (Bressler and Menon, 2010; Bullmore and Sporns, 2012; Menon, 2011; Rubinov and Sporns, 2010; Smith, 2012).

In line with the recent emphasis on large-scale network models, the current analysis addresses two gaps in the current literature regarding

* Corresponding author at: 6001 Research Park Blvd, Madison, WI 53719, United States.
E-mail address: jcisler2@wisc.edu (J.M. Cisler).

the brain mechanisms impacted by early life trauma. First, there is limited existing data regarding the association between early life trauma and large-scale network organization. One prior study linked pediatric PTSD with a greater clustering coefficient (i.e., fraction of a node's neighbors that are neighbors of each other, averaged across the network) and a higher average path length during resting-state (Suo et al., 2015) using a relatively small brain parcellation of 90 regions-of-interest (ROIs). Nonetheless, the association between severity of early life trauma and large-scale network organization, to our knowledge, has not yet been investigated.

Second, and relatedly, it is not clear how nodal findings specified in neurocircuitry models of trauma and PTSD (Admon et al., 2013), such as amygdala hyperactivity or amygdala-medial PFC functional connectivity, fit into large-scale network models. That is, from a network perspective, the relevant behavior to consider revolves around the interactions between large populations of nodes and the sub-modules that they comprise. By contrast, the neurocircuitry models of trauma and PTSD seem to focus on the behavior of a few nodes without considering their role(s) in the larger brain network. For example, consider the role of amygdala hyperactivity or weakened amygdala-mPFC connectivity within the context of modularity, a key organizing principle of complex systems (Hartwell et al., 1999; Newman, 2003, 2006). Modularity refers to the degree to which a network is comprised of functionally specialized modules, is broadly characterized by greater within-module connectivity compared to between-module connectivity, and is formally defined as the difference between the observed within module connections and that expected by chance (Hartwell et al., 1999; Newman, 2006). If early life trauma is associated with amygdala hyperactivity or weakened amygdala-mPFC connectivity, how might these nodal findings affect overall network modular organization? Conversely, if the behavior of specific nodes within a network is driven in a top-down manner by large-scale network organization, then observed associations between early life trauma and specific nodal behavior may be better understood by characterizing the large-scale organization network patterns that produce the specific nodal behavior. If this is the case, then it is indeed important to characterize the association, if any, between early life trauma and large-scale network organization, and it is equally important to test the association between large-scale network organization and common nodal findings implicated in early life trauma and PTSD, such as amygdala hyperactivity and weakened connectivity between amygdala and mPFC (Garrett et al., 2012; Dannlowski et al., 2012; Wolf and Herringa, 2016; Cisler et al., 2013). As it stands, the literature regarding the brain mechanisms impacted by early life trauma and the literature regarding large-scale brain network organization are largely independent. The goal of the current analysis is to begin to integrate these lines of research.

Towards these larger goals, we use graph theory analyses to characterize large-scale network organization during emotion processing among a relatively large sample of adolescent girls. We characterize functional network organization during a facial emotion processing task similar to variants used in this literature to observe amygdala hyperactivation among trauma-exposed individuals (Bryant et al., 2008; Rauch et al., 2000; Williams et al., 2006a). While much research demonstrates amygdala hyperactivation to threat compared to neutral faces among trauma exposed individuals (Rauch et al., 2006; Bryant et al., 2008; Williams et al., 2006a), it is noteworthy that studies of trauma and PTSD also find amygdala hyperactivation to neutral faces as well (Garrett et al., 2012; Hendler et al., 2003; Brunetti et al., 2010), perhaps suggesting a generalization of threat processing in the amygdala. Therefore, we characterize large-scale network organization to not only the contrast of fear compared to neutral emotion processing, but also to the main effect of facial emotional processing per se. Consistent with recent analyses of network organization in PTSD (Suo et al., 2015; Cisler et al., 2016; Spielberg et al., 2015) and neuroimaging in general (Rubinov and Sporns, 2010; Bullmore and Sporns, 2009), we utilize concepts and analytical approaches from graph theory to

characterize large-scale brain network organization.

Based on prior network studies in pediatric PTSD demonstrating greater clustering coefficients (Suo et al., 2015), a measure of segregated information processing, and our previous finding that greater modularity during fear processing predicts better PTSD symptom reduction (Cisler et al., 2016), we hypothesize a scalar relationship between early life trauma and modularity, assortativity, and global efficiency. We additionally hypothesize that individual differences in large-scale network organization during the task will be predictive of amygdala functional activation and amygdala-mPFC connectivity during the task.

2. Materials and methods

2.1. Participants

Adolescent girls, aged 11 to 17, were recruited as part of three separate studies from 2011 to 2016. Two studies investigated the neural correlates of early life assaultive violence exposure and one study investigated the neural correlates of treatment response among adolescent girls with PTSD related to physical or sexual assault, but the current analysis does not repeat prior published reports (Cisler et al., 2013, 2015, 2016) from these data (see Supplemental material for description of previous published results using these data). Healthy controls were recruited based on the absence of current mental health disorders, psychiatric medication use, developmental disorders, and history of trauma exposure. Assaulted adolescent girls were enrolled based on history of self-reported physical or sexual abuse and the absence of developmental disorders or MRI contraindications. See Supplemental material for further exclusion criteria and details. Demographic and clinical characteristics are depicted in Table 1. Following removal of 6 participants due to excessive head motion (see below), the final sample consisted of 88 participants.

All participants' mental health was assessed with either the K-SADS (Kaufman et al., 1997) ($n = 30$) or MINI-KID (Sheehan et al., 2010) ($n = 58$). Both are widely used structured clinical interviews for most Axis I disorders found in childhood and adolescence. Assaultive trauma histories were characterized using the trauma assessment section of the

Table 1
Demographic and clinical characteristics.

Variable	Control ($n = 29$)	Assault ($n = 59$)	Group difference p value
	Mean/ frequency (SD)	Mean/ frequency (SD)	
Age	14.97 (1.8)	14.6 (1.69)	0.35
Ethnicity	58% Caucasian 34% African American 0% Hispanic 3% Biracial 3% Other	50% Caucasian 40% African American 3% Hispanic 3% Biracial 2% Other	0.50
Verbal IQ	108.9 (20.5)	97.4 (14.4)	0.003
Mean age of first assault	NA	8.40 (4.00)	–
Mean age of last assault	NA	12.02 (3.36)	–
Total number of types of direct assaults	0	3.4 (2.6)	–
Physical assault	–	98.3%	–
Sexual assault	–	48.3%	–
Childhood Trauma Questionnaire	41.1 (7.79)	57.1 (17.8)	< 0.001
PTSD symptom severity	–	29.04 (17.85)	–
SFMQ total	3.6 (3.2)	10.0 (7.7)	< 0.001
Current PTSD	0%	64%	–

Note. Depression severity in adolescents measured with Short Mood and Feelings Questionnaire (SMFQ). PTSD severity in adolescents measured with UCLA PTSD Reaction Index.

National Survey of Adolescents (NSA) (Kilpatrick et al., 2000; Kilpatrick et al., 2003), a structured interview used in prior epidemiological studies of assault and mental health functioning among adolescents that uses behaviorally specific dichotomous questions to assess sexual assault, physical assault, severe abuse from a caregiver, and witnessed violence. Participants also completed a more inclusive assessment of childhood maltreatment via the Childhood Trauma Questionnaire (CTQ) (Bernstein and Fink, 1998), a widely used self-report measure assessing separate physical abuse, physical neglect, emotional abuse, emotional neglect, and sexual abuse domains of childhood trauma. Analyses here focused on the CTQ total score across all domains. We focus primary analyses on the CTQ, given that primary findings in the field related to early life trauma have used this measure (Dannowski et al., 2012; Heringa et al., 2013). The assessments also included measures of verbal IQ (receptive one word picture vocabulary test (Brownell, 2000)), PTSD symptom severity (UCLA PTSD Reaction Index (Steinberg et al., 2004, 2013)), and depression severity (Short Mood and Feelings Questionnaire (Angold et al., 1995); SMFQ).

2.2. MRI acquisition

For 58 participants ($n = 44$ directly assaulted adolescents, $n = 14$ healthy controls), a Philips 3 T Achieva X-series MRI system with a 32-channel head coil (Philips Healthcare, USA) was used to acquire imaging data. Anatomic images were acquired with a MPRAGE sequence (matrix = 256×256 , 160 sagittal slices, TR/TE/FA = 2600 ms/3.02 ms/80°, final resolution = $1 \times 1 \times 1 \text{ mm}^3$ resolution). Echo planar imaging (EPI) sequences were used to collect the functional images using the following sequence parameters: TR/TE/FA = 2000 ms/30 ms/90°, FOV = $240 \times 240 \text{ mm}$, matrix = 80×80 , 37 oblique slices (parallel to AC-PC plane to minimize OFC signal artifact), slice thickness = 2.5 mm with a 0.5 mm gap between slices, re-sampled during preprocessing to a final resolution = $3 \times 3 \times 3 \text{ mm}^3$.

For 30 participants ($n = 15$ directly assaulted adolescents, $n = 15$ healthy controls), image acquisition parameters were slightly different. An 8-channel head coil was used to acquire the imaging data. Anatomic images were collected using identical sequences and parameters. The EPI images were collected using identical parameters except slice thickness was 3 mm and collected with an interleaved sequence. Despite differences in head coils, all participants were scanned on the same scanner.

Importantly for the present analyses, image acquisition methodology was not correlated with CTQ ($r = 0.06$, $p = 0.55$). As detailed below, we conducted additional analyses to support combining data across head coil cohorts and to rule out the possibility that the observed effects are due to differences in the head coil.

2.3. Image preprocessing

Image preprocessing followed standard steps and was completed using AFNI software. In the following order, images underwent despiking, slice timing correction, deobliquing, motion correction using rigid body alignment, alignment to participant's normalized anatomical images, spatial smoothing using a 8 mm FWHM Gaussian filter (AFNI's 3dBlurToFWHM that estimates the amount of smoothing to add to each dataset to result in the desired level of final smoothing), detrending, low frequency (128 s) bandpass filtering, and rescaling into percent signal change. Images were normalized using the MNI 152 template brain. Following recent recommendations (Power et al., 2014; Siegel et al., 2014), we corrected for head motion related signal artifacts by using motion regressors derived from Volterra expansion, consisting of $[R R^2 R_t - 1 R_t^2 - 1]$, where R refers to each of the 6 motion parameters, and separate regressors for mean signal in the CSF and WM. This step was implemented directly after motion correction and normalization of the EPI images in the image preprocessing stream. Additionally, we censored TRs from the first-level GLMs based on threshold of framewise

displacement (FD) > 0.5 . FD refers to the sum of the absolute value of temporal differences across the 6 motion parameters; thus, a cut-off of 0.5 results in censoring TRs where the participant moved, in total across the 6 parameters, more than $\sim 0.5 \text{ mm}$ plus the immediately following TR (to account for delayed effects of motion artifact). Additionally, we censored isolated TRs where the preceding and following TRs were censored, and we censored entire runs if $> 50\%$ of TRs within that run were censored. Mean FD was 0.16 (SD = 0.09), which was unrelated to CTQ and direct assaults ($t_s < 1.39$, $p_s > 0.17$).

2.4. Implicit threat processing task

The emotion processing task used here was similar to that used in prior research (Bryant et al., 2008; Rauch et al., 2000; Williams et al., 2006b). Participants made button presses indicating decisions related to the sex of the poser while viewing human faces taken from the NimStim facial stimuli set. The faces contained either neutral or fearful expressions, presented either overtly or covertly, in alternating blocks. There were an equal number of female and male faces. Overt faces were presented for 500 ms, with a 1200 ms inter-stimulus-interval displaying a blank screen with a fixation cross, in blocks of 8 presentations for a total block length of $\sim 17 \text{ s}$. Covert face blocks used a similar design but were presented for 33 ms followed immediately by a neutral facial expression mask for 166 ms from the same actor depicted in the covert image, and the ISI was 1500 ms. Rest blocks that displayed a blank screen with a fixation cross and lasted 10 s were additionally included. The task was presented in two runs, each lasting $\sim 8 \text{ min}$, during which each block type was presented 5 times. There were 10 total blocks for each stimulus category.

2.5. fMRI data analysis

2.5.1. Defining task-specific network properties

Our methodology for characterizing patterns of large-scale organization of functional connectivity during the task was as described in our previous report among treatment-seeking adolescent girls with PTSD (Cisler et al., 2016), and we summarize the methodology here. A full description is in Supplemental material. After omitting ROIs compromised by individual differences in spatial coverage (e.g., some participants did not have complete coverage in the cerebellum) and signal dropout (e.g., signal dropout in the OFC), 783 ROIs of the total 883 ROIs in the parcellation (Craddock et al., 2012) were retained that were shared across all participants. Rather than calculating the correlation between ROIs using the full timeseries, we are interested in functional connectivity specific to the facial emotion processing conditions and therefore focus on functional connectivity specific to each stimulus condition for each of the 783 ROIs. This was computed using the beta series method (Rissman et al., 2004; Cisler et al., 2014), in which a separate beta coefficient is estimated for each unique block across each voxel, resulting in 10 beta coefficients for each voxel for each stimulus condition. We then extracted the mean timeseries of beta coefficients, representing activity to each block presentation, across the voxels within each of 783 ROIs, separately for each stimulus condition. These series of beta coefficients were then correlated separately for each stimulus condition. Next, network indices were calculated on each of the r -to- z transformed connectivity matrices separately. We used the Brain Connectivity Toolbox (Rubinov and Sporns, 2010) implemented in Matlab.

2.5.2. Defining group-level community structure of the brain during emotion processing

Full details are included in Supplemental material. We characterized the group-level community structure of the 783 ROIs using a similar methodology described above, except that we calculated the square correlation matrices for each participant collapsed across stimulus categories, and then created a group-level connectivity matrix by

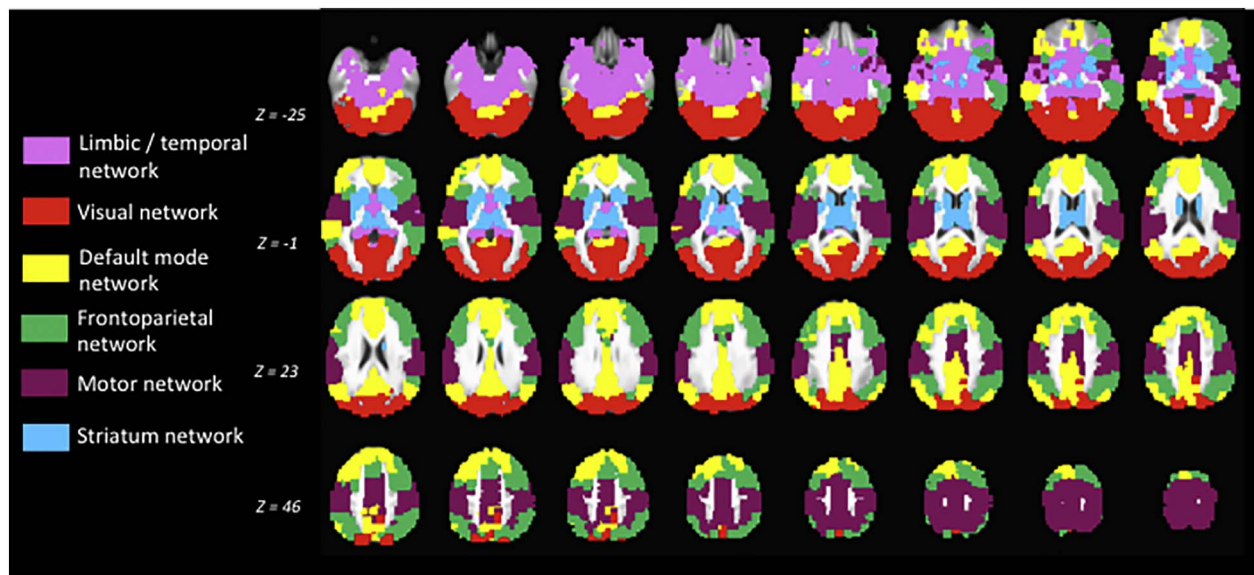


Fig. 1. Graphical depiction of the group-level large-scale modular brain organization observed during the task collapsed across stimulus conditions.

taking the median connectivity values across participants, resulting in a single 783×783 connectivity matrix. This community structure is depicted in Fig. 1.

2.5.3. Relationship between childhood maltreatment, clinical symptoms, and network organization

We tested for scalar relationships between large-scale functional brain organization and childhood trauma among all participants with regression models, in which the network index of interest was regressed simultaneously onto 1) CTQ total score, 2) ethnicity, 3) verbal IQ, 4) age, and 5) head motion (mean framewise displacement). Ethnicity, verbal IQ, age, and head motion are included as covariates to remove any variance in network organization related to these factors to allow more precise estimates regarding the effect of early life trauma. These analyses were repeated using the network indices collapsed across all stimuli (main effect of face processing on network organization) as well as for the contrast of fear vs neutral (network organization differences between fear and neutral stimuli). To correct for family-wise multiple comparisons, we set alpha to 0.0167 (i.e., $0.05/\text{number of family-wise comparisons}$). Post-hoc tests are explicitly labeled and provide uncorrected p values.

2.5.4. Relationship between network organization and functional activation

To identify relationships between large-scale functional brain organization and voxelwise functional activation, we first characterized functional brain activation using standard first level analyses resulting in spatial maps of beta coefficients for each task conditions. Full details are included in Supplemental material. Next, second-level analyses consisted of voxelwise regression models in which each voxel's contrast estimate was regressed onto the network index of interest as well as the covariates of age, ethnicity, verbal IQ, and head motion. We maintained a corrected $p < 0.05$ using cluster-level thresholding (3dClustSim) and estimating observed spatial smoothing using the spatial autocorrelation function to account for the recently observed false positive rates associated with an assumed Gaussian distribution of spatial smoothing (Eklund et al., 2016). With an uncorrected voxelwise threshold of $p < 0.005$, a cluster size of 36 contiguous voxels (nearest neighbor = 1) yielded a corrected $p < 0.05$.

2.5.5. Relationship between network organization and amygdala-mPFC functional activation

Following the identification of bilateral amygdala clusters (see

below) related to large-scale network organization, we tested for task-related functional connectivity of these clusters with a mPFC ROI independently chosen from a separate study showing decreased amygdala-rostral ACC functional connectivity during threat image viewing among a pediatric PTSD sample (Wolf and Herringa, 2016). The mPFC ROI consisted of an 8 mm sphere centered on the coordinates of: $X = 0$, $Y = 46$, $Z = 12$. The beta series timecourses from the amygdala and mPFC ROIs were separately correlated for each task condition for each participant. Regression analyses then tested whether amygdala-mPFC functional connectivity was related to network organization, again controlling for age, ethnicity, verbal IQ, and head motion.

3. Results

3.1. Modular brain organization during facial emotion processing

Fig. 1 illustrates the group-level community structure identified during the task collapsed across all task conditions. As can be seen, the algorithm detected distinct functional modules that seem visually consistent with the canonical networks of the frontoparietal network, motor network, default mode network, limbic/temporal lobe network, striatal network, and visual network.

3.2. Relationship between early life trauma and large-scale network organization

We first tested the relationship between early life trauma and large-scale functional network organization collapsed across all stimulus categories (main effect of facial emotion processing). These analyses (Fig. 2, top panel) revealed that, when controlling for head motion, age, ethnicity, and verbal IQ, early life trauma was strongly associated with greater modularity ($t = 4.2$, $p < 0.001$), greater assortativity ($t = 4.1$, $p < 0.001$), and lessor global efficiency ($t = -3.16$, $p = 0.002$). As can be seen in Fig. 2 (lower panel), these relationships were consistent across stimulus categories. Indeed, there was no relationship between the contrast of fear vs neutral facial emotion processing for any of the network indices (all p s > 0.6). Supplemental Fig. 1 displays a heat map separately for the high and low CTQ groups (based on median split) to provide a visualization of the differences in the topology of the large-scale functional network organization.

We also conducted post-hoc comparisons of the clinical group of adolescent girls directly physically or sexually assaulted and healthy

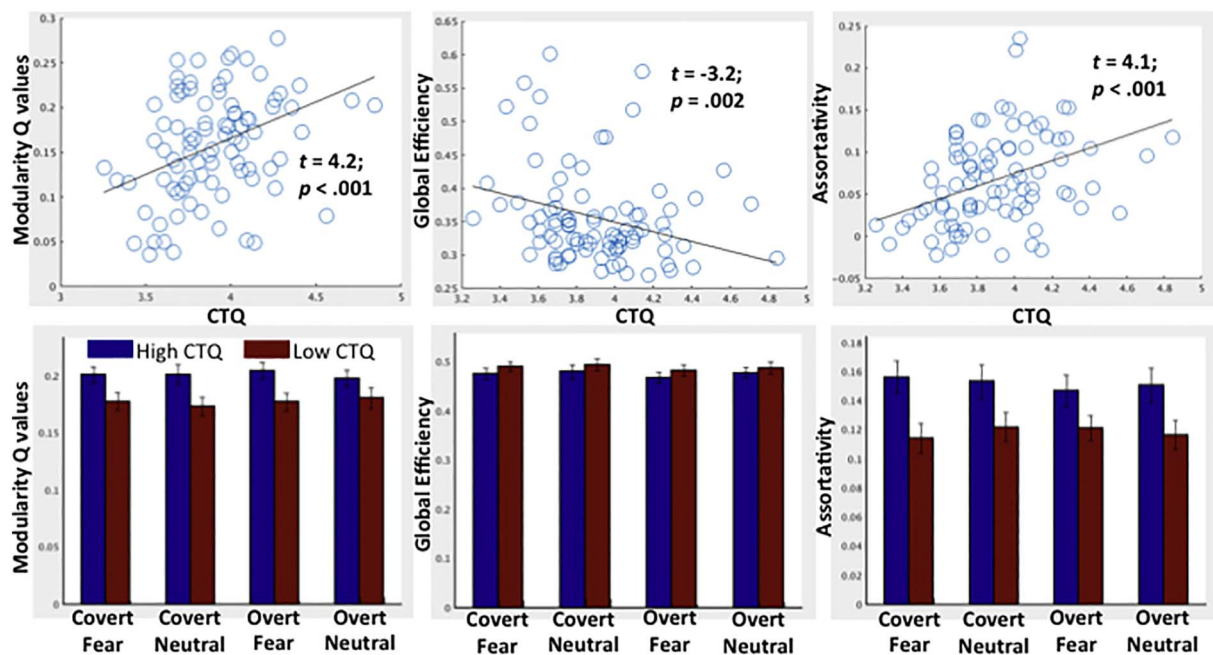


Fig. 2. Top) scatter plots depicting the relationship between CTQ (log transformed) and network modularity, assortativity, and global efficiency. B coefficients and p values come from regression models that also include age, ethnicity, verbal IQ, and head motion as covariates. Bottom) Bar graphs comparing high and low CTQ groups, based on median split, on network modularity, assortativity, and global efficiency separately for each task condition. Error bars denote standard error.

control girls to corroborate the scalar relationship between CTQ and network organization across all stimulus categories. We observed that the assaulted adolescent girls demonstrated greater overall modularity ($t = 2.07, p = 0.041$) and assortativity ($t = 2.20, p = 0.025$), but no differences in global efficiency, when again controlling for the above mentioned covariates. Twenty-two of the assaulted girls were taking a psychotropic medication, which was unrelated to all of the network indices across all stimulus categories (all t s < 1.2 , p s > 0.24).

As an additional post-hoc analysis, we also tested whether, among the adolescent girls exposed to direct physical or sexual assault ($n = 58$), CTQ continued to predict altered network organization when controlling for PTSD symptom severity. When including PTSD symptom severity as an additional covariate, CTQ continued to significantly predict greater modularity ($t = 2.28, p = 0.027$), greater assortativity ($t = 2.37, p = 0.022$), and marginally lesser global efficiency ($t = -1.93, p = 0.060$). While PTSD symptom severity was not related to any of the network indices when controlling for CTQ (all t s < 1.22 , p s > 0.23), dichotomous PTSD diagnoses were significantly associated with greater modularity Q values ($t = 2.05, p = 0.045$) when controlling for CTQ, but not with assortativity or global efficiency (t s < 1 , p s > 0.37). Similarly, depression severity was not associated with the network indices when controlling for CTQ (all t s < 1.3 , p s > 0.20), while CTQ remained a significant predictor of modularity ($t = 3.23, p = 0.0018$), assortativity ($t = 4.02, p < 0.001$), and marginally so for global efficiency ($t = -1.86, p = 0.067$).

3.3. Relationship between large-scale network organization and functional activation during facial emotion processing

We next tested the degree to which individual differences in modularity values, collapsed across all task conditions, were related to individual differences in voxelwise functional activation during the task, again collapsed across all task conditions. Controlling for age, ethnicity, verbal IQ, and head motion, we observed among the entire sample ($N = 88$) significant positive relationships between network modularity Q values and functional activation in bilateral amygdala (Supplemental Fig. 2; full functional activation results are provided in Supplemental Table 1). Given that the clusters observed here extend

laterally outside of the amygdala, we also placed 4 mm spherical ROIs specifically within the amygdala-sites of these clusters to aid in interpretability of the amygdala specifically. These ROIs were centered at XYZ MNI coordinates of 20, -2 , -20 , and -24 , -1 , -19 . The correspondence between these amygdala-specific ROIs and the clusters identified from the whole-brain analysis with modularity is depicted in Supplemental Fig. 2. When repeating the analyses using the mean activity within these specific ROIs, we again observed significant positive relationships with modularity Q values (Fig. 3).

We next conducted post-hoc analyses to replicate prior effects related to the CTQ and amygdala activation in the current data. We observed significant positive relationships between CTQ and left amygdala activation ($t = 2.4, p < 0.019$), and a statistical trend with right amygdala activation ($t = 1.89, p < 0.063$) (Fig. 4), when controlling for the above mentioned covariates and using the amygdala-specific ROIs. To confirm amygdala engagement to the task, we tested the degree to which these amygdala ROIs were active to the main effect of face processing. As expected, both the right ($t = 3.47, p = 0.001$) and left ($t = 2.37, p = 0.02$) amygdala ROIs were significantly positively engaged during face processing.

3.4. Relationship between large-scale network organization and amygdala-mPFC functional connectivity

We next tested whether individual differences in modularity values across all stimulus conditions were similarly related to amygdala-mPFC functional connectivity across all stimulus conditions using the beta series method of functional connectivity (Rissman et al., 2004; Cisler et al., 2014). The mPFC ROI was chosen from an independent study among a pediatric PTSD sample (Wolf and Herringa, 2016), and we used the amygdala-specific ROIs described above to aid in inferences regarding the amygdala specifically. Controlling for the above-mentioned covariates, we observed that modularity Q values collapsed across stimulus conditions were significantly negatively correlated with functional connectivity between mPFC and both right ($t = -3.00, p = 0.003$) and left ($t = -2.1, p = 0.038$) amygdala collapsed across stimulus conditions (Fig. 4). However, we observed no significant relationships between CTQ and amygdala-mPFC functional connectivity

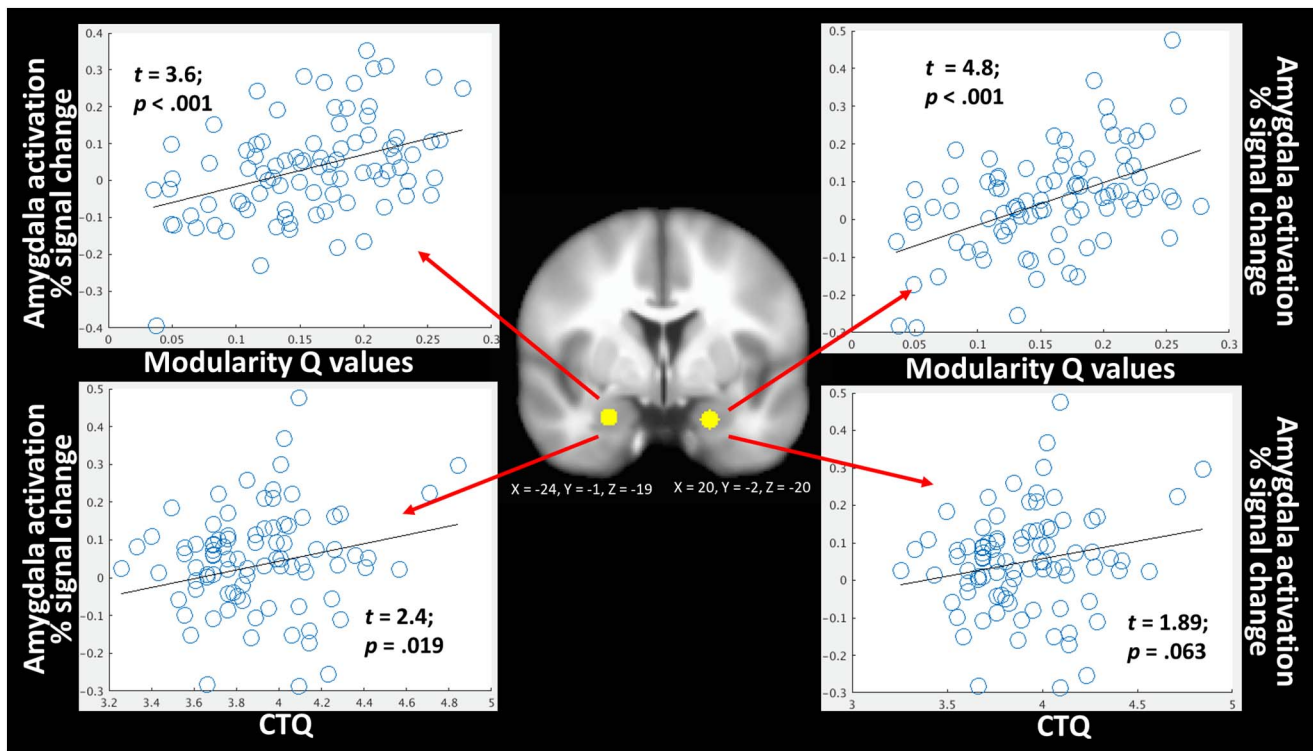


Fig. 3. Graphical depiction of the bilateral amygdala clusters where functional activation during all facial emotion conditions was predicted by network modularity Q values (top left and right). These amygdala clusters were similarly significantly related to severity of CTQ (log transformed). *B* coefficients and *p* values come from regression models that also include age, ethnicity, verbal IQ, and head motion as covariates.

(*ps* > 0.16).

4. Discussion

We observed here that severity of self-reported early life trauma was strongly associated with enhanced modular and assortative network organization, and decreased global efficiency, during facial emotion processing independent of the valence or stimulus presentation duration of the emotional expression. We similarly observed that girls directly physically or sexually assaulted also demonstrated more modular and assortative network organization compared to control adolescents. Further, among these assaulted girls, the relationships with early life trauma remained when controlling for PTSD symptom severity, suggesting that the effects reflect the extent of trauma exposure and not

simply current clinical severity. There was additional evidence, that above and beyond the effect of CTQ, PTSD diagnoses among the assaulted girls were associated with greater modularity, suggesting a role for modular brain organization in psychopathology following early life trauma.

We also observed that individual differences in large-scale network modularity were predictive of both the degree of bilateral amygdala functional activation during the task as well as degree of functional connectivity between the amygdala and mPFC. While we did not observe that the effects regarding amygdala activation were constrained to threat processing, hyperactive amygdala towards neutral stimuli among PTSD and trauma victims is commonly observed (Garrett et al., 2012; Hendler et al., 2003; Brunetti et al., 2010). Importantly, we were also able to replicate prior effects of positive associations between early

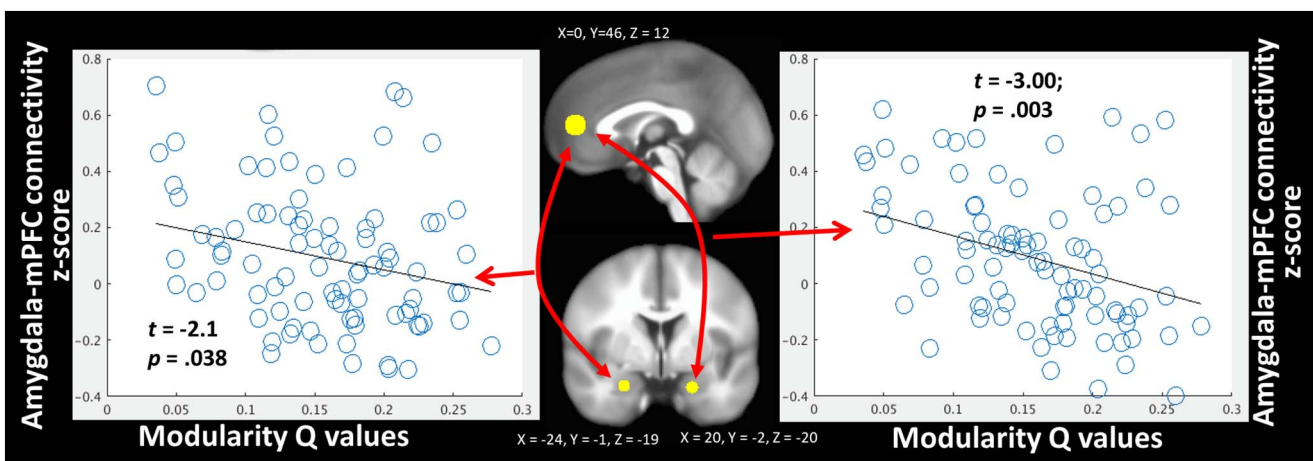


Fig. 4. Graphical depiction of the relationships between bilateral amygdala and mPFC connectivity with network modularity Q values collapsed across all stimuli. *B* coefficients and *p* values come from regression models that also include age, ethnicity, verbal IQ, and head motion as covariates.

life trauma and amygdala activation (Dannlowski et al., 2012) and positive amygdala activation to the face processing task (Johnson, 2005), which provides an indication of external validity to these data.

These results have implications for our understanding of the neural mechanisms by which early life trauma confers risk for psychopathology. Most neurocircuitry models of PTSD and trauma emphasize functional activation or connectivity within a constrained set of regions implicated in threat processing and emotion regulation/fear inhibition (Pitman et al., 2012; Rauch et al., 2006; Admon et al., 2013). At the same time, contemporary neuroimaging approaches emphasize a network-level conceptualization of brain function (Smith, 2012; Bullmore and Sporns, 2009; Smith et al., 2009; Sporns et al., 2004) and utilize concepts from network science to understand organization and development of the human brain (Rubinov and Sporns, 2010; Chen and Deem, 2015; Godwin et al., 2015; Gu et al., 2015; Meunier et al., 2009). To our knowledge, there have not been prior efforts testing the degree to which node-specific findings discussed in neurocircuitry models are related to measures of large-scale organization. By demonstrating that PTSD-related node-specific effects are related to large-scale brain organization patterns, the current results provide support for a model positing broader effects of early life trauma on large-scale functional network organization (Patel et al., 2012). It is tempting to hypothesize a top-down model, such that previously reported findings of hyperactive amygdala and weakened amygdala-mPFC connectivity among trauma-exposed samples are actually due to higher-order differences in network organization. For example, perhaps the amygdala hyperactivity is a downstream product of the ability of the network to rapidly organize into a modularized structure, thus allowing more specialized and enhanced processing of faces. Similarly, perhaps the weakened amygdala-mPFC connectivity reflects that these nodes are part of separate functionally specialized modules (see Fig. 1); thus, when the overall network organizes into a modularized structure, the degree of connectivity between these two nodes necessarily decreases.

However, it is important to note that the current cross-sectional study cannot establish directional causality and that a bottom-up process, whereby amygdala hyperactivity and weakened amygdala-mPFC connectivity drive the altered organization of the larger network, is also possible. Indeed, animal models demonstrate that chronic stressor exposure and/or chronic glucocorticoid administration affects neuronal density and branching of specific nodes with the canonical PTSD and trauma neurocircuitry (Mcewen, 2004; Roozendaal et al., 2009; Vyas et al., 2002). Further, a recent study using designer receptors exclusively activate by designer drugs (DREADDS) among non-human primates found that inactivation of the amygdala was associated with large-scale changes in network organization (Grayson et al., 2016). From this perspective, one might hypothesize that larger-scale changes in brain organization may indeed be driven by changes in local nodes. It seems clear that a top-down vs bottom-up conceptualization of the relationship between node-specific effects and network organization patterns leads to different predictions and clinical implications. Future research is needed to further characterize the relationships between node-specific findings and larger patterns of brain organization.

Several limitations must nonetheless temper inferences from the current study. First, the sample was limited to all girls, and it is not clear how these results would generalize to boys. Second, our findings linking large-scale network organization to functional activation results are limited to facial emotion processing. As such, we cannot rule out the alternative hypothesis that early life trauma enhanced network organization during active task engagement per se, as opposed to the more specific inference for face processing. Third, our clinical sample of assaulted adolescent girls was not psychotropic medication-free, and while we did not observe any associations between network organization and medication use, inferences must nonetheless be tempered. Fourth, portions of the data were collected with different head coils, and while we conducted additional analyses to rule out head coil differences as a confound (see Supplementary material), heterogeneity

introduced by the head coil differences can nonetheless not be ruled out. Fifth, we chose an mPFC ROI from a prior study of pediatric PTSD (Wolf and Herringa, 2016), and while this ROI overlaps spatially with meta-analytic findings of amygdala-pgACC connectivity disruptions associated with internalizing symptoms (Marusak et al., 2016), the ROI used here was slightly more anterior and dorsal. Finally, we did not include a measure of socioeconomic status and cannot rule out any effect of this variable on CTQ or the brain measures of interest.

Supplementary data to this article can be found online at <https://doi.org/10.1016/j.nicl.2017.12.001>.

Funding and disclosures

Portions of this work were supported by grants R21MH106860, K08MH100267, T32DA022981, and R21MH097784. All authors report no conflicts of interest.

References

- Admon, R., Milad, M.R., Hendler, T., 2013. A causal model of post-traumatic stress disorder: disentangling predisposed from acquired neural abnormalities. *Trends Cogn. Sci.* 17, 337–347.
- Angold, A., Costello, E.J., Messer, S.C., Pickles, A., 1995. Development of a short questionnaire for use in epidemiological studies of depression in children and adolescents. *Int. J. Methods Psychiatr. Res.* 5 (4), 237–249.
- Bernstein, D.P., Fink, L., 1998. *Childhood Trauma Questionnaire: A Retrospective Self-report: Manual*. Harcourt Brace & Company.
- Bressler, S.L., Menon, V., 2010. Large-scale brain networks in cognition: emerging methods and principles. *Trends Cogn. Sci.* 14, 277–290.
- Brownell, R., 2000. *Receptive One-word Picture Vocabulary Test: Manual*. Academic Therapy Publications.
- Brunetti, M., et al., 2010. Elevated response of human amygdala to neutral stimuli in mild post traumatic stress disorder: neural correlates of generalized emotional response. *Neuroscience* 168, 670–679.
- Bryant, R.A., et al., 2008. Enhanced amygdala and medial prefrontal activation during nonconscious processing of fear in posttraumatic stress disorder: an fMRI study. *Hum. Brain Mapp.* 29, 517–523.
- Bullmore, E., Sporns, O., 2009. Complex brain networks: graph theoretical analysis of structural and functional systems. *Nat. Rev. Neurosci.* 10, 186–198.
- Bullmore, E., Sporns, O., 2012. The economy of brain network organization. *Nat. Rev. Neurosci.* 13, 336–349.
- Chen, M., Deem, M.W., 2015. Development of modularity in the neural activity of children's brains. *Phys. Biol.* 12, 16009.
- Cisler, J.M., et al., 2011a. PTSD symptoms, potentially traumatic event exposure, and binge drinking: a prospective study with a national sample of adolescents. *J. Anxiety Disord.* 25, 978–987.
- Cisler, J.M., et al., 2011b. A prospective examination of the relationships between PTSD, exposure to assaultive violence, and cigarette smoking among a national sample of adolescents. *Addict. Behav.* 36, 994–1000.
- Cisler, J.M., et al., 2012. Exposure to interpersonal violence and risk for PTSD, depression, delinquency, and binge drinking among adolescents: data from the NSA-R. *J. Trauma. Stress.* 25, 33–40.
- Cisler, J.M., Scott Steele, J., Smitherman, S., Lenow, J.K., Kilts, C.D., 2013. Neural processing correlates of assaultive violence exposure and PTSD symptoms during implicit threat processing: a network-level analysis among adolescent girls. *Psychiatry Res.* 214, 238–246.
- Cisler, J.M., Bush, K., Steele, J.S., 2014. A comparison of statistical methods for detecting context-modulated functional connectivity in fMRI. *NeuroImage* 84, 1042–1052.
- Cisler, J.M., et al., 2015. Amygdala response predicts trajectory of symptom reduction during trauma-focused cognitive-behavioral therapy among adolescent girls with PTSD. *J. Psychiatr. Res.* 71, 33–40.
- Cisler, J.M., et al., 2016. Modes of large-scale brain network organization during threat processing and posttraumatic stress disorder symptom reduction during TF-CBT among adolescent girls. *PLoS One* 11, e0159620.
- Craddock, R.C., James, G.A., Holtzheimer, P.E., Hu, X.P., Mayberg, H.S., 2012. A whole brain fMRI atlas generated via spatially constrained spectral clustering. *Hum. Brain Mapp.* 33, 1914–1928.
- Dannlowski, U., et al., 2012. Limbic scars: long-term consequences of childhood maltreatment revealed by functional and structural magnetic resonance imaging. *Biol. Psychiatry* 71, 286–293.
- Eklund, A., Nichols, T.E., Knutsson, H., 2016. Cluster failure: why fMRI inferences for spatial extent have inflated false-positive rates. *Proc. Natl. Acad. Sci.* 113, 7900–7905.
- Felitti, V.J., et al., 1998. Relationship of childhood abuse and household dysfunction to many of the leading causes of death in adults. *Am. J. Prev. Med.* 14, 245–258.
- Garrett, A.S., et al., 2012. Brain activation to facial expressions in youth with PTSD symptoms. *Depress. Anxiety* 29, 449–459.
- Godwin, D., Barry, R.L., Marois, R., 2015. Breakdown of the brain's functional network modularity with awareness. *Proc. Natl. Acad. Sci.* 112, 3799–3804.
- Grayson, D.S., et al., 2016. The rhesus monkey connectome predicts disrupted functional

- networks resulting from pharmacogenetic inactivation of the amygdala. *Neuron* 91, 453–466.
- Green, J., McLaughlin, K.A., Berglund, P.A., et al., 2010. Childhood adversities and adult psychiatric disorders in the national comorbidity survey replication I: associations with first onset of DSM-IV disorders. *Arch. Gen. Psychiatry* 67, 113–123.
- Gu, S., et al., 2015. Emergence of system roles in normative neurodevelopment. *Proc. Natl. Acad. Sci.* 112, 13681–13686.
- Hartwell, L.H., Hopfield, J.J., Leibler, S., Murray, A.W., 1999. From molecular to modular cell biology. *Nature* 402, C47–C52.
- Hendler, T., et al., 2003. Sensing the invisible: differential sensitivity of visual cortex and amygdala to traumatic context. *NeuroImage* 19, 587–600.
- Herrington, R.J., et al., 2013. Childhood maltreatment is associated with altered fear circuitry and increased internalizing symptoms by late adolescence. *Proc. Natl. Acad. Sci.* 110, 19119–19124.
- Johnson, M.H., 2005. Subcortical face processing. *Nat. Rev. Neurosci.* 6, 766–774.
- Kaufman, J., et al., 1997. Schedule for affective disorders and schizophrenia for school-age children-present and lifetime version (K-SADS-PL): initial reliability and validity data. *J. Am. Acad. Child Adolesc. Psychiatry* 36, 980–988.
- Kilpatrick, D.G., et al., 2000. Risk factors for adolescent substance abuse and dependence: data from a national sample. *J. Consult. Clin. Psychol.* 68, 19–30.
- Kilpatrick, D.G., et al., 2003. Violence and risk of PTSD, major depression, substance abuse/dependence, and comorbidity: results from the National Survey of Adolescents. *J. Consult. Clin. Psychol.* 71, 692–700.
- Marusak, H.A., et al., 2016. You say ‘prefrontal cortex’ and I say ‘anterior cingulate’: meta-analysis of spatial overlap in amygdala-to-prefrontal connectivity and internalizing symptomatology. *Transl. Psychiatry* 6, tp2016218.
- McEwen, B.S., 2004. Protection and damage from acute and chronic stress: allostasis and allostatic overload and relevance to the pathophysiology of psychiatric disorders. *Ann. N. Y. Acad. Sci.* 1032, 1–7.
- McLaughlin, K.A., et al., 2010. Childhood adversities and adult psychiatric disorders in the national comorbidity survey replication II: associations with persistence of DSM-IV disorders. *Arch. Gen. Psychiatry* 67, 124–132.
- Menon, V., 2011. Large-scale brain networks and psychopathology: a unifying triple network model. *Trends Cogn. Sci.* 15, 483–506.
- Meunier, D., Achard, S., Morcom, A., Bullmore, E., 2009. Age-related changes in modular organization of human brain functional networks. *NeuroImage* 44, 715–723.
- Newman, M.E.J., 2003. The structure and function of complex networks. *SIAM Rev.* 45, 167–256.
- Newman, M.E.J., 2006. Modularity and community structure in networks. *Proc. Natl. Acad. Sci.* 103, 8577–8582.
- Patel, R., Spreng, R.N., Shin, L.M., Girard, T.A., 2012. Neurocircuitry models of post-traumatic stress disorder and beyond: a meta-analysis of functional neuroimaging studies. *Neurosci. Biobehav. Rev.* 36, 2130–2142.
- Pitman, R.K., et al., 2012. Biological studies of post-traumatic stress disorder. *Nat. Rev. Neurosci.* 13, 769–787.
- Power, J.D., et al., 2014. Methods to detect, characterize, and remove motion artifact in resting state fMRI. *NeuroImage* 84, 320–341.
- Rauch, S.L., et al., 2000. Exaggerated amygdala response to masked facial stimuli in posttraumatic stress disorder: a functional MRI study. *Biol. Psychiatry* 47, 769–776.
- Rauch, S.L., Shin, L.M., Phelps, E.A., 2006. Neurocircuitry models of posttraumatic stress disorder and extinction: human neuroimaging research—past, present, and future. *Biol. Psychiatry* 60, 376–382.
- Rissman, J., Gazzaley, A., D’Esposito, M., 2004. Measuring functional connectivity during distinct stages of a cognitive task. *NeuroImage* 23, 752–763.
- Roozendaal, B., McEwen, B.S., Chattarji, S., 2009. Stress, memory and the amygdala. *Nat. Rev. Neurosci.* 10, 423–433.
- Rubinov, M., Sporns, O., 2010. Complex network measures of brain connectivity: uses and interpretations. *NeuroImage* 52, 1059–1069.
- Sheehan, D.V., et al., 2010. Reliability and validity of the mini international neuropsychiatric interview for children and adolescents (MINI-KID). *J. Clin. Psychiatry* 71, 313–326.
- Siegel, J.S., et al., 2014. Statistical improvements in functional magnetic resonance imaging analyses produced by censoring high-motion data points. *Hum. Brain Mapp.* 35, 1981–1996.
- Smith, S.M., 2012. The future of fMRI connectivity. *NeuroImage* 62, 1257–1266.
- Smith, S.M., et al., 2009. Correspondence of the brain’s functional architecture during activation and rest. *Proc. Natl. Acad. Sci.* 106, 13040–13045.
- Spielberg, J.M., McGlinchey, R.E., Milberg, W.P., Salat, D.H., 2015. Brain network disturbance related to posttraumatic stress and traumatic brain injury in veterans. *Biol. Psychiatry* 78, 210–216.
- Sporns, O., Chialvo, D.R., Kaiser, M., Hilgetag, C.C., 2004. Organization, development and function of complex brain networks. *Trends Cogn. Sci.* 8, 418–425.
- Steinberg, A.M., et al., 2013. Psychometric properties of the UCLA PTSD reaction index: part I. *J. Trauma. Stress.* 26, 1–9.
- Steinberg, A.M., Brymer, M.J., Decker, K.B., Pynoos, R.S., 2004. The University of California at Los Angeles post-traumatic stress disorder reaction index. *Curr. Psychiatry Rep.* 6 (2), 96–100.
- Suo, X., et al., 2015. Disrupted brain network topology in pediatric posttraumatic stress disorder: a resting-state fMRI study. *Hum. Brain Mapp.* 36, 3677–3686.
- Vyas, A., Mitra, R., Rao, B.S.S., Chattarji, S., 2002. Chronic stress induces contrasting patterns of dendritic remodeling in hippocampal and amygdaloid neurons. *J. Neurosci.* 22, 6810–6818.
- Williams, L.M., et al., 2006a. Trauma modulates amygdala and medial prefrontal responses to consciously attended fear. *NeuroImage* 29, 347–357.
- Williams, L.M., et al., 2006b. Amygdala–prefrontal dissociation of subliminal and supraliminal fear. *Hum. Brain Mapp.* 27, 652–661.
- Wolf, R.C., Herrington, R.J., 2016. Prefrontal–amygdala dysregulation to threat in pediatric posttraumatic stress disorder. *Neuropsychopharmacology* 41, 822–831.